Transp Porous Med (2011) 90:333–362
DOI 10.1007/s11242-011-9788-8

Oil Recovery by Low Salinity Water Injection into a Reservoir: A New Study of Tertiary Oil Recovery Mechanism

Y. Li

Received: 26 July 2010 / Accepted: 30 May 2011 / Published online: 24 June 2011

Abstract Low salinity water injections for oil recovery have shown seemingly promising results in the case of clay-bearing sandstones saturated with asphaltic crude oil. Reported data showed that low salinity water injection could provide up to 20% pore volume (PV) of additional oil recovery for core samples and up to 25% PV for reservoirs in near wellbore regions, compared with brine injection at the same Darcy velocity. The question remains as to whether this additional recovery is also attainable in reservoirs. The answer requires a thorough understanding of oil recovery mechanism of low salinity water injections. Numerous hypotheses have been proposed to explain the increased oil recovery using low salinity water, including migration of detached mixed-wet clay particles with absorbed residual oil drops, wettability alteration toward increased water-wetness, and emulsion formation. However, many later reports showed that a higher oil recovery associated with low salinity water injection at the common laboratory flow velocity was neither necessarily accompanied by migration of clay particles, nor necessarily accompanied by emulsion. Moreover, increased water-wetness has been shown to cause the reduction of oil recovery. The present study is based on both experimental and theoretical analyses. Our study reveals that the increased oil recovery is only related to the reduction of water permeability due to physical plugging of the porous network by swelling clay aggregates or migrating clay particles and crystals. At a fixed apparent flow velocity, the value of negative pressure gradient along the flow path increases as the water permeability decreases. Some oil drops and blobs can be mobilized under the increased negative pressure gradient and contribute to the additional oil recovery. Based on the revealed mechanism, we conclude that low salinity water injection cannot be superior to brine injection in any clay-bearing sandstone reservoir at the maximum permitted injection pressure. Through our study of low salinity water injection, the theory of tertiary oil recovery has been notably improved.

Keywords Low salinity · Tertiary recovery · Oil mobilization · Water permeability · Clay plugging

Y. Li (✉)
Department of Chemical and Petroleum Engineering, University of Wyoming, Laramie, WY 82071, USA
e-mail: liyu9826@hotmail.com

List of Symbols

BR	Brine injection
BT	Breakthrough
Ca	Dimensionless capillary number
D_c	Core diameter (m)
DW	Distilled water injection
EOR	Enhanced oil recovery
f'	Derivative of water fractional flow with respect to water saturation (df/dS_w)
f'_f	Derivative of water fractional flow with respect to water saturation at the water-invading front
HF	High flow rate injection
K	Absolute permeability (air permeability) (m^2)
K_w	Permeability of the water phase (m^2)
k_{rw}	Relative permeability to the water phase
L	Length of the bypass (m)
L_c	Length of the core (m)
LS	Low salinity brine injection
N_c	Standard capillary number (m^{-2})
N_c^0	Standard capillary number at the tertiary oil recovery of 7.3% PV for the core with $\theta_R = 0$ (m^{-2})
P_1	Upstream pressure (Pa)
P_2	Downstream pressure (Pa)
P_{cb}	Back capillary pressure (Pa)
P_{cf}	Frontal capillary pressure (Pa)
P_{cP}	Capillary pressure generated by the interface in the pore (Pa)
P_{cT}	Capillary pressure generated by the interface in the throat (Pa)
P_{ST}/P_{PT}	Ratio of snap-off capillary pressure in a throat to capillary pressure for the piston-like advance of a convex interface in the same throat
PV	Pore volume (m^3)
q_w	Volumetric flow rate of water (m^3/s)
r_P	Pore radius (m)
r_T	Throat radius (m)
r_P/r_T	Pore–throat aspect ratio
S_{oi}	Initial oil saturation
S_{ro}	Residual oil saturation
S_w	Water saturation
S_{wi}	Initial water saturation
TDS	Total dissolved solids (kg/m^3)
V	Darcy velocity (apparent velocity) (q_w/A) (m/s)
V_w	Cumulative volume of the injected water (m^3)
V_{wBT}	Cumulative water injection volume at water breakthrough (m^3)
x	Distance (m)
ΔP	Injection pressure difference (Pa)
ΔP^*	Injection pressure difference corresponding to final tertiary oil recovery for each core (Pa)
$\Delta P_w/\Delta x$	Gradient of pressure in the water (Pa/m)
ΔQ_o	Increased oil recovery in PV during a period of water injection
ΔQ_o^*	Final tertiary oil recovery in PV for each core
ϕ	Core porosity

μ Viscosity (Pa.s)
μ_w Water viscosity (Pa.s)
μ_0 Oil viscosity (Pa.s)
θ_A Advancing contact angle (°)
θ_R Receding contact angle (°)
σ Interfacial tension (N/m)
ζ Ratio of N_c to N_c^*

1 Introduction

Increased oil recovery can be obtained by injection of low salinity water for clay-bearing sandstone cores or clay-bearing sandstone formations in near wellbore regions, compared with brine injection at the same Darcy velocity, according to the reports (Tang and Morrow 1997, 1999; Webb et al. 2004, 2005; McGuire et al. 2005; Zhang and Morrow 2006; Lager et al. 2006, 2007; Loahardjo et al. 2007). Up to now, the reported field data are still from the formations in near wellbore regions, where the calculated tertiary oil recovery associated with low salinity water injection is very high (20–25% pore volume, PV). However, the near-well data are not representative of the field conditions distant from wellbores. Unexpectedly, in a recent report the increased oil recovery associated with low salinity water injection in the laboratory was as high as that in near wellbore regions. (Loahardjo et al. 2007)

Many hypotheses have been proposed to explain the oil recovery mechanism of low salinity water injections. Those included migration of detached mixed-wet clay particles with absorbed residual oil drops (Tang and Morrow 1999), wettability alteration toward increased water-wetness (Tang and Morrow 1999; Ligthelm et al. 2009; Austad and Puntervold 2010; Sorbie and Collins 2010), saponification (McGuire et al. 2005), and cation exchange (Lager et al. 2006; Lebedeva et al. 2009; Austad and Puntervold 2010). However, none of these hypotheses has been verified by experiments.

Therefore, we carried out a new study based on systematic experiments under the guidance of the basic theories associated with secondary and tertiary oil recoveries. The underlying enhanced oil recovery (EOR) mechanism of low salinity water injections was verified to be the mobilization of discontinuous oil, which occurs under a negative pressure gradient higher than that during the brine injection at the same flow velocity, as water permeability is reduced due to blockage of the porous network by swelling clay aggregates or migrating clay particles and crystals. The study revealed that for a clay-bearing sandstone reservoir, the increased oil recovery associated with injection of low salinity water is dependent on flow velocity and flow acceleration. Thus, the increased recovery associated with low salinity water injection from a clay-bearing sandstone reservoir will be significantly less than that from the reservoir core at the common laboratory flow velocity. The study also revealed that during low salinity injections the increased oil recovery (at the same flow velocity) is outweighed by two relevant disadvantages, the reduced water injectivity and degraded mobilization condition. Thus, for any clay-bearing sandstone reservoir, the oil recovery associated with low salinity water injection cannot be higher than that associated with brine injection at the maximum permitted injection pressure.

2 Theory

Primary oil recovery is performed without injections. Subsequently, there are two modes of oil recoveries associated with injections, i.e., secondary oil recovery and tertiary oil recov-

ery. However, secondary oil recovery may start without a primary oil recovery operation in practice. Secondary oil recovery for a homogeneous reservoir is likely to be as high as that for the reservoir cores at low flow velocity (the dimensionless capillary number (Ca) corresponding to the low flow rate should be less than 10^{-3} for the strongly water-wet bead packs with permeability of 13–17 μm^2 (Wardlaw 1988), for example) but this is not true for tertiary oil recovery associated with water injection. The estimation of tertiary oil recovery associated with water injection from a reservoir should be based on the experimental dependence on the flow velocity and flow acceleration. The discrepancy results because secondary oil recovery frequently originates from continuous oil phase while tertiary oil recovery always originates from discontinuous oil phase. The disconnection of continuous oil phase in secondary oil recovery is related to snap-off of selloidal interfaces, which is independent of flow velocity at low capillary number, while mobilization of discontinuous oil in tertiary oil recovery associated with water injection is related to pressure gradient, which is dependent on flow velocity at any capillary number higher than the critical.

It should be pointed out that snap-off may be dependent on flow velocity at high capillary number, due to less convex interfaces arriving at the pores with pore–throat ratios higher than the critical. This is not the case discussed above.

However, there are a few cases where secondary oil recovery comes from both continuous and discontinuous oil phases (secondary oil recovery associated with low salinity water injection from clay-bearing sandstone at common experimental flow rate, for example). Therefore, to verify whether a part of secondary oil recovery also comes from the discontinuous oil phase, laboratory tests at lower flow rates must be conducted. The fundamental mechanisms of secondary and tertiary oil recoveries are described below.

2.1 Fundamentals in Secondary Oil Recovery

Discussed here are the cases where secondary oil recovery comes only from the continuous oil phase during water injections. The fundamental theory on secondary oil recovery was proposed by Li and Wardlaw (1986a,b). The study showed that the disconnection of oil by snap-off of a selloidal interface in a pore depends on the pore–throat aspect ratio (r_P/r_T), wettability, and supply of water (Fig. 1). The critical pore–throat aspect ratio for a pore is the ratio above which snap-off will happen in the pore when water is supplied at least to one of its throats. A further study (Li et al. 1986) showed that secondary oil recovery depends on the following factors: pore and throat size distributions and their size correlation, ratio of throat numbers to pore numbers, initial water saturation, and wettability. For two similar cores with the same wettability, oil recovery will be higher for the core with lower initial water saturation; for two similar cores with the same initial water saturation, oil recovery will be higher for the core with stronger oil-wetness. The influence of wettability on secondary oil recovery will be explained as follows. As we know, there is always a water-invading front during secondary oil recovery and the continuous oil phase ahead of the front must be disconnected by snap-off to permit water moving forward. For a more-water-wet core, occurrence of snap-off is easier due to the relatively low critical pore–throat aspect ratio. Hence, more oil disconnections can occur at and behind the water-invading front, and higher oil recovery at water breakthrough (BT) will be obtained from this core. However, for a more-oil-wet core, occurrence of snap-off is more difficult due to the relatively high critical pore–throat aspect ratio. Therefore, much of continuous oil phase can be preserved for a longer time to permit more continuous oil branches withdrawing from porous channels in a piston-like manner. As a result, higher final oil recovery will be obtained from the more-oil-wet core.

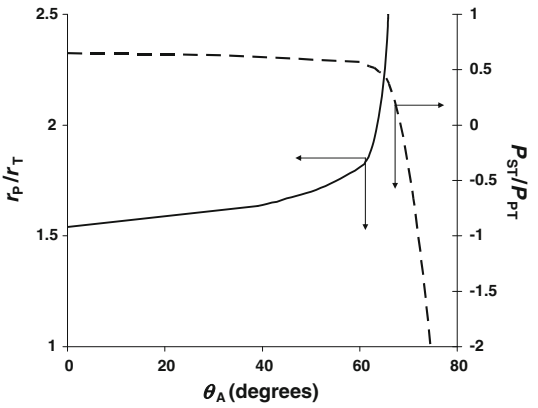

Fig. 1 Critical pore–throat aspect ratio (r_P/r_T) versus advancing contact angle (θ_A) (according to Li and Wardlaw 1986a,b). The ratio of snap-off capillary pressure in a throat to capillary pressure for the advance of a convex interface in the same throat (P_{ST}/P_{PT}) is the reciprocal of pore–throat aspect ratio (r_P/r_T). The critical P_{ST}/P_{PT} is on the broken line

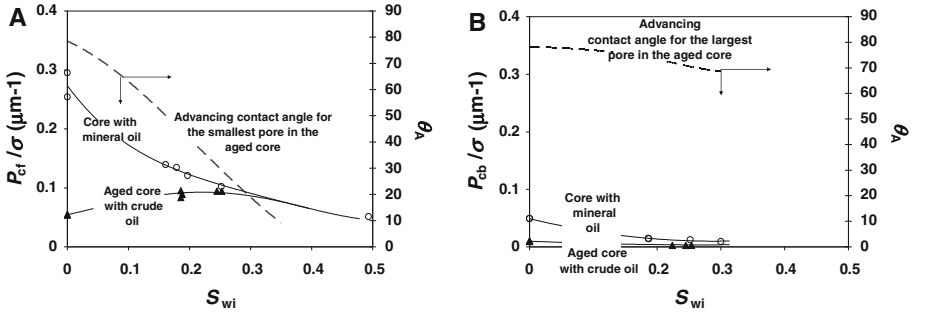

Fig. 2 Measurement of advancing contact angle inside cores (according to Li 2010). The results are obtained from Berea sandstone with permeability (K) of about 0.9 μm^2. P_{cf}/σ is the curvature of the interface at the water- invading front (**a**) and P_{cb}/σ is the curvature of the interface at the core open face (**b**). θ_A represents the advancing contact angles. S_{wi} is the initial water saturation

The conclusion was established when 3-D two-phase flow simulations in the porous network were performed for the first time (Li et al. 1986).

Li et al. introduced the measurement of the end pressure during the restricted and unrestricted counter-current spontaneous imbibitions in order to measure the frontal capillary pressures and calculate the back capillary pressures (Li et al. 2006; Ligthelm et al. 2009). Recently, Li obtained the analytical solutions of counter-current spontaneous imbibition in the frontal flow period (Li 2011). Since then, the determination of contact angles as a function of pore sizes inside a core has become possible, as long as a comparison of the capillary pressures is made between the core under investigation and a very strongly water-wet core with the same lithology and initial water saturation (Fig. 2).

As the parameters at the water-invading front were eventually determined by Li (2010), obtaining the accurate Buckley-Leverett saturation profiles during forced water injections has become possible. The key formula for determining the water-invading front is obtained directly from the relationship between the derivative of water fractional flow with respect to saturation at the outlet of the core ($f' = \mathrm{d}f/\mathrm{d}S_w$) and the cumulative injected water volume (V_w) at the moment of water BT:

$$f'_f = \frac{1}{V_{wBT}}, \tag{1}$$

where f'_f is the derivative of water fractional flow with respect to saturation (f') corresponding to the water-invading front and V_{wBT} is the cumulative injected water volume (V_w) in PV at BT. The relation between f' and V_w at the outlet of the core was obtained by Welge (1952).

As the influences of wettability and initial water saturation on secondary oil recovery are incorporated in the saturation profile, the above technical progress makes these influences demonstrable. The demonstration using the data in this article will be displayed in the Sect. 5.

2.2 Fundamentals in Tertiary Oil Recovery Associated with Water Injection

Unlike secondary oil recovery, the oil phase distributes discontinuously in the pore network during tertiary oil recovery. The discontinuous oil phase is in the form of drops (in single pores) or blobs (extending over many adjacent pores), which have been trapped in pore networks due to capillary pressure actions. This phenomenon is called Jamin effect, named after a work by Jamin a long time ago (Jamin 1860). To let trapped drops and blobs move, mechanical work must be provided externally or surface energy must be reduced internally, or both. The stimulation of oil in tertiary oil recovery is called the mobilization of residual oil in petroleum terminology. Tertiary oil recovery is also called EOR in the oil industry. However, the increased oil recovery due to mobilization of discontinuous oil in secondary oil recovery will be also called EOR in later descriptions. Sometimes, ground water and petroleum researchers and engineers relate mobilization of a gas bubble or an oil drop to the dimensionless capillary number (Ca) (Gardescu 1930; Moore and Slobod 1956; Melrose and Brandner 1974), which is expressed as:

$$Ca = \frac{\mu V}{\sigma}, \tag{2}$$

where μ is the viscosity of the displacing phase (water, in most cases), V is the apparent velocity (Darcy velocity) of the injected (displacing) phase (water, in most cases), and σ is the interfacial tension between the displacing phase and the displaced phase (water and gas or water and oil, in most cases). The above formula is suitable for the very strongly water-wet system in which the water permeability does not apparently change during water injections. According to the reports, the critical Ca for onset of mobilization is 10^{-3} to 10^{-5} for the water-wet glass-bead and sand packing (Wardlaw 1988) and 7×10^{-6} to 2×10^{-7} for the water-wet sandstone cores. (Chatzis and Morrow 1984). As well, the Ca for complete oil recovery is about 10^{-2}. For tertiary oil recovery associated with water injection, the capillary number should be redefined to satisfy the requirements of oil reservoir applications.

The redefinition of capillary number will be based on the elemental capillary-trap model as shown in Fig. 3.

For the capillary-trap model, we assume that the investigated oil drop completely blocks the downstream throat. Therefore, P_1 is the pressure in the water phase at the upstream convex interface and P_2 is the pressure in the water phase at the downstream convex interface.

The Young–Laplace's equation for the downstream convex interface is

$$P_{cT} = \frac{2\sigma \cos\theta_R}{r_T}, \tag{3}$$

where P_{cT} is the capillary pressure generated by the convex interface in the downstream throat, r_T is the radius of the downstream throat, σ is the interfacial tension between oil and water, and θ_R is the receding contact angle.

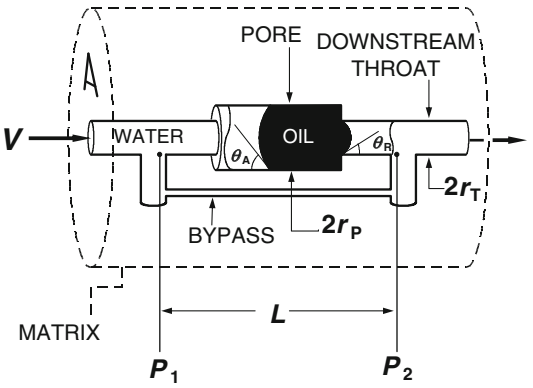

Fig. 3 The elemental model of capillary trap for explaining the tertiary oil recovery mechanism. The cross sections of all capillary tubes are circular. V is the flow rate through a unit area (A) of the matrix (porous medium) which contains the elemental trap. P_1 is the upstream pressure in water which is exerted on the convex interface in the pore. P_2 is the downstream pressure in water which is exerted on the convex interface in the throat. L is the length of the bypass. θ_A represents the advancing contact angles and θ_R represents the receding contact angles

The Young–Laplace's equation for the upstream convex interface is

$$P_{cP} = \frac{2\sigma \cos\theta_A}{r_P} = \frac{2\sigma \cos\theta_R}{r_P(\cos\theta_R/\cos\theta_A)}, \tag{4}$$

where P_{cP} is the capillary pressure generated by the convex interface in the pore, r_P is the radius of the pore, and θ_A is the advancing contact angle.

Subtracting both sides of Eq. 4 from those of Eq. 3, we obtain:

$$P_{cT} - P_{cP} = \left(\frac{1}{r_T} - \frac{1}{r_P(\cos\theta_R/\cos\theta_A)}\right) 2\sigma \cos\theta_R. \tag{5}$$

As shown by the model, the equation for the critical equilibrium will be:

$$P_1 - P_2 = -(P_{cT} - P_{cP}). \tag{6}$$

Combining Eqs. 5 and 6 yields:

$$P_1 - P_2 = \left(\frac{1}{r_P(\cos\theta_R/\cos\theta_A)} - \frac{1}{r_T}\right) 2\sigma \cos\theta_R. \tag{7}$$

To investigate the mobilization of an oil drop in the elemental capillary-trap model, we need the generalized Darcy's law for the water phase:

$$V = \frac{q_w}{A} = -\frac{Kk_{rw}}{\mu_w}\frac{\Delta P_w}{\Delta x} = -\frac{K_w}{\mu_w}\frac{\Delta P_w}{\Delta x}, \tag{8}$$

where q_w is the volumetric flow rate of water, A is the cross-sectional area of the core or the matrix which contains the elemental capillary-trap complex, $V(= q_w/A)$ is the Darcy velocity (apparent velocity), K is the absolute permeability of the core or the porous matrix, k_{rw} is the relative permeability to the water phase, $K_w(= Kk_{rw})$ is the permeability of the water phase, μ_w is the water viscosity, P_w is the pressure in water phase, and x is the distance.

If the cross sections of the bypass capillary tube are assumed uniform, the pressure gradient in water, $\Delta P_w/\Delta x$, will be expressed as:

$$\frac{\Delta P_w}{\Delta x} = \frac{(P_1 - P_2)}{L}, \tag{9}$$

where L is the length of the bypass.

Combining Eqs. 7, 8, and 9 yields:

$$V = \frac{K_w}{\mu_w}\left(\frac{1}{r_T} - \frac{1}{r_P(\cos\theta_R/\cos\theta_A)}\right)\frac{1}{L}2\sigma\cos\theta_R \tag{10}$$

or

$$2\left(\frac{1}{r_T} - \frac{1}{r_P(\cos\theta_R/\cos\theta_A)}\right)\frac{1}{L} = \frac{\mu_w V}{K_w\sigma\cos\theta_R}. \tag{11}$$

Expressed as the same dimensions [M^{-2}] as those of the reciprocal of permeability, the left-hand side of Eq. 11 shows the resistance against mobilization of residual oil. Therefore, the left-hand side of Eq. 11 deserves being named as the standard capillary number (N_c) and Eq. 11 then becomes:

$$N_c = \frac{\mu_w V}{K_w\sigma\cos\theta_R}. \tag{12}$$

On the other hand, the right-hand side of Eq. 12 (or Eq. 11) represents the dynamic value for mobilization of the trapped oil in the capillary trap.

Let us find the physical meaning of the investigated terms. The left-hand side of Eq. 11 describes the geometry of the capillary barrier, which is characterized by r_T and r_P of the main-pass, and L of the bypass (corresponding to the length of no-flow segment in main-pass). For the same wettability, if the throat diameter is smaller, the pore diameter is bigger, or the length of no-flow segment is shorter in the main-pass, the resistance against mobilization in the trap will be higher. Also, the hysteresis of the contact angle ($\cos\theta_R/\cos\theta_A$) has an apparent influence on the resistance against mobilization in the trap. When the contact angle is about 60° in the same trap, the resistance against mobilization in the trap will be the highest; when the contact angle is close of 90° in the same trap, the resistance against mobilization in the trap may be zero. Therefore, an oil drop cannot be mobilized until a higher dynamic value is exceeded for the same trap with weak water-wetness. The left-hand side of Eq. 11 also indicates that the initial oil distribution of tertiary oil recovery must have a strong influence on the relation between tertiary oil recovery and the standard capillary number. The initial oil distribution is related to the pore structure, initial and residual water saturation of secondary oil recovery, so that the pattern of the oil traps must be different for a different initial oil distribution of tertiary oil recovery. Alternatively, the right-hand side of Eq. 11 represents the detailed dynamics for mobilization of the trapped oil. Lower interfacial tension, stronger oil-wetness, lower water permeability, higher water viscosity, or higher flow velocity always leads to a higher dynamic value of the standard capillary number (N_c).

The comprehensive character of pore structure and oil distribution is quantitatively defined by the newly introduced variable K_w and the wettability is quantitatively defined by another newly introduced variable θ_R. Three variables (V, μ_w, and σ) previously introduced in the formula of dimensionless capillary number (Ca) deal only with the behaviors of the fluids. Therefore, the standard capillary number (N_c) is the comprehensive criteria for analyzing any kind of tertiary oil recovery. In the tertiary oil recovery practice, the capillary force, $\sigma\cos\theta_R$, can be effectively reduced by lowering interfacial tension during injection of water

accompanied by hydrocarbon solvents or surfactants; the viscous force, $\mu_w V/K_w$, has to be carefully adjusted by limiting injection flow rate not too high, otherwise the over elevated pressure gradient ($\Delta P_w/\Delta_x$) may cause hydro-fracturing in the flooded formation. This can be simply concluded by the formula: $N_c = (\Delta P_w/\Delta_x)/(\sigma \cos\theta_R)$, which is the combination of Eq. 12 and Eq. 8.

The newly introduced variable K_{w}, the permeability of the water phase, may change as oil saturation is reduced or water channels are plugged (by polymer or clay, for example) or dredged (by acidization, for example). Besides, the oil viscosity (μ_o) may have influence during oil drops flows, but the value of K_w can include its effect. It should be pointed out that for any trap in the porous network, its main-pass may become a bypass for another coming oil drop and its bypass may become a main-pass for another coming oil drop. Therefore, when water permeability is decreased, some or all traps in the porous network become harsher at the same time.

Wardlaw and McKellar (1985) observed that the larger oil blobs were disconnected repeatedly during mobilization. It can also be found from their elaborate distributions where the sizes of blobs decreased with subsequent increases in capillary number. Therefore, we may anticipate that the increment of tertiary oil recovery associated with water injection for the same infinitesimal N_{c} is less for more-oil-wet cores, because the disconnection by snap-off is more difficult in more-oil-wet pores (Li and Wardlaw 1986a,b).

In Sect. 5, the tertiary oil recovery associated with low salinity water injection will be quantitatively analyzed in terms of all dynamic variables of the standard capillary number, especially in terms of the two newly introduced variables: water permeability and wettability.

3 Experiments

3.1 Materials

3.1.1 Mineral Oil

A refined mineral oil (Soltrol 220) with viscosity of 3.9 mPa s and density of 0.783 g/ml was used for establishing the very strongly water-wet core test. Polar contaminants in the mineral oil were removed by flowing through a packed column of silica and alumina gel.

3.1.2 Crude Oil

An asphaltic crude oil (Cottonwood Crude Oil) with viscosity of 24.3 mPa s and density of 0.887 g/ml was used for establishing the weakly water-wet to very weakly water-wet cores. The properties of asphaltenes in the crude oil are shown in Table 1. The crude oil was filtered to remove solid particles and then evacuated for 24 h to avoid gas production during water injections.

Table 1 Asphaltenes in crude oil

Crude oil	Cottonwood
n-C_7 asphaltenes (wt%)	2.3
Acid # (mg KOH/g oil)	0.56
Base # (mg KOH/g oil)	1.83

3.1.3 Brine and Low Salinity Water

The used brine was synthetic seawater (35,540 parts of million (ppm) of total dissolved solids (TDS)) with the composition shown in Table 2. The viscosity of brine was about 1.0 mPa s at 22°C. The density of brine was 1.02 g/ml at 22°C.

In our experiments, two kinds of low salinity water were injected. One was 20 times diluted synthetic seawater (1,780 ppm), which we called low salinity brine. The other was the distilled water (0 ppm). For reference, two values are given as follows. The salinity of low salinity water is less than 6,000 ppm; the salinity of fresh water is less than 500 ppm.

All types of water used in the tests were degassed by evacuation before injections.

The interfacial tension (σ) between the mineral oil and brine was 48.8 mN/m and the interfacial tension (σ) between the crude oil and brine was 29.7 mN/m.

3.1.4 Cores

The cores were drilled from a block of Berea sandstone which contains about 6% kaolinite and few other clay minerals. The core diameters (D_c) ranged from 3.63 to 3.67 cm and the core lengths (L_c) ranged from 6.23 to 6.48 cm. The permeability to air (K) ranged from 0.648 to 0.695μm^2 and the porosity (ϕ) ranged from 21.3 to 21.4% (see Table 3).

3.2 Establishment of Initial Water Saturation

The lateral surface of each cylindrical core was sealed with a segment of heat-shrinkable Teflon tube before the establishment of initial saturation. Core BW0 was completely saturated with brine first and then injected with 100 ml of mineral oil at the flow rate of 0.3 ml/min at 22°C to establish the initial water saturation (S_{wi}). Core BW1 was completely saturated with brine first and then injected with 100 ml of asphaltic crude oil at the flow rate of 0.3 ml/min at 22°C to establish the initial water saturation. Core BW2 was completely saturated with brine first and a large part of brine was then displaced by nitrogen, which was eventually displaced by crude oil in the vacuum at 22°C. Core BW3 was completely saturated with crude oil in the vacuum at 22°C.

3.3 Aging

After establishing the initial water saturations, those cores saturated with crude oil were submerged in the filtered crude oil in the sealed pressure vessels and aged at 75°C exactly for 10 days.

Table 2 Brine composition

Salt	Composition (g/l)
NaCl	28.00
KCl	0.94
$CaCl_2$	1.18
$MgCl_2$	5.42
TDS	35.54

Table 3 Core size, porosity, and permeability

Core	L_c (cm)	D_c (cm)	ϕ (%)	K (μm^2)
BW0	6.48	3.67	21.3	0.648
BW1	6.45	3.64	21.3	0.686
BW2	6.35	3.63	21.3	0.656
BW3	6.23	3.64	21.4	0.695

Aging is a rapid experimental procedure for obtaining the similar asphaltene deposits on the mineral surfaces, as obtained under the reservoir temperature and pressure for a geological time. The measurements (Fig. 2) show that the asphaltene deposits can cause the cores more oil-wet.

4 Experimental Results

To reveal the oil recovery mechanism of low salinity water injections, the experiments were meticulously designed. The tested rock is Berea sandstone, which contains clay. The chosen cores are almost identical in size, porosity, and permeability. The lateral surface of any tested cylindrical core was sealed with heat-shrinkable Teflon tube to ensure the water injection performance to be strict one-dimensional two-phase flow at a constant flow rate (Li 2010). The chosen crude oil is an asphaltic crude oil. Crude oil saturations of 0–100% were established in cores to control the wettability from very strong water-wetness to very weak water-wetness. Except for a high flow water injection, all water injections were conducted at the flow rate of 0.3 ml/min at 22°C in order to make the comparisons easier. The salinity varied in a very broad range, 35,540–0 ppm, for detecting the reduction of water permeability due to plugging of porous network by swelling or migrating clay. Necessary measurements, such as brine injection after distilled water injection and high flow rate injection after low flow rate injection, were conducted to make further investigations. Although, the tests were conducted under room temperature and atmospheric pressure, the resulting relationships between oil recovery and dynamic variables are representative for brine and low salinity water injections in clay-bearing sandstone.

It should be stated that in our experiments, the EOR was also obtained by injection of low salinity water from the core completely saturated with asphaltic crude oil or only saturated with mineral oil at the common laboratory flow rate.

4.1 Secondary Oil Recovery Associated with Injection of Brine

4.1.1 Wettability in the Tested Samples

The systematic wettability measurements for Berea sandstone with permeability of about 0.9 μm^2 had been completed based on the data of the end pressures of spontaneous imbibitions (Fig. 2) (Li 2010). Considering that the same wettability almost corresponds to the same initial water saturation (S_{wi}) for Berea sandstone with permeability of about 0.07 μm^2, the contact angles for our tested samples were assigned according to their S_{wi} and listed in Table 4. The medians of advancing contact angles were 0°, 48°, 61°, and 78° for cores BW0, BW1, BW2, and BW3, respectively.

Table 4 Core wettability

Core	Oil	σ (mN/m)	S_{wi} (%)	Data for $K = 0.9\ \mu m^2$			
				P_{cf}/σ (μm^{-1})	P_{cb}/σ (μm^{-1})	θ_A (°)	Median of θ_A (°)
BW0	Mine.	48.8	26.6	0.1013	0.0105	0	0
BW1	Crude	29.7	27.2	0.0900	0.0035	25–70	48
BW2	Crude	29.7	19.1	0.0919	0.004	47–74	61
BW3	Crude	29.7	0	0.0548	0.01	78	78

Table 5 Brine injections

Core	Oil	Water	V_w		ΔQ_o (%)	ΔP (kPa)	S_{ro} (%)
			(ml)	(PV)			
BW0	Mine.	Sea water	185	12.7	27.3	15.6	46.1
BW1	Crude	Sea water	263	18.6	34.0	10.0	38.8
BW2	Crude	Sea water	370	26.4	35.4	12.3	45.5
BW3	Crude	Sea water	370	26.7	56.5	3.4	43.5

4.1.2 Brine Injection Performances

Seawater (35,540 ppm) injections were conducted at a constant water injection rate (q_w) of 0.3 ml/min at 22°C. The injected volumes of brine (V_w) were 185–370 ml (12.7–26.7 PVs) to ensure no further oil production from the cores (Fig. 4 and Table 5). High recovery was obtained from the very weakly water-wet core without initial water saturation (BW3). Intermediate recoveries were obtained from the weakly water-wet cores with initial water saturations (BW2 and BW1). Low recovery was obtained from the very strongly water-wet cores with initial water saturations (BW0). Secondary oil recoveries (ΔQ_o) in PV were 27.3, 34.0, 35.4, and 56.5% from cores BW0, BW1, BW2, and BW3, respectively. The injection pressure differences (ΔP) were 15.5, 10.0, 12.3, and 3.4 kPa at the residual oil saturations (S_{or}) for the respective cores. No clay fines were produced.

4.2 Tertiary Oil Recovery Associated with Injections of Water with Different Low Salinity

4.2.1 Low Salinity Brine Injections

Injections of low salinity brine (1,780 ppm) at a constant water injection rate (q_w) of 0.3 ml/min at 22°C were conducted after brine injections terminated (Fig. 5 and Table 6). The effluents during the tertiary oil recovery operations were collected by other separators. The injected volumes of low salinity brine (V_w) were 360–446 ml (25.4–29.3 PVs) to ensure no further oil production from the cores. High increased recovery was obtained from the very weakly water-wet core without initial water saturation (BW3). Intermediate increased recoveries were obtained from the weakly water-wet cores with initial water saturations (BW2 and BW1). No recovery was obtained from the very strongly water-wet core with initial water

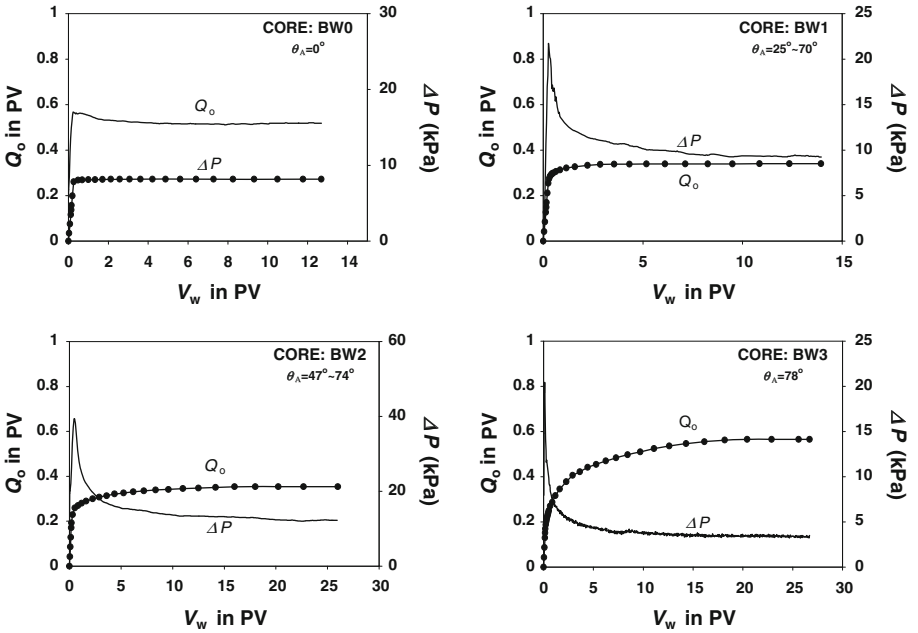

Fig. 4 Performance of the secondary oil recovery associated with brine injection. V_w is the cumulative volume of injected brine in PV and Q_o is the oil recovery in PV. ΔP is the injection pressure difference. θ_A represents the advancing contact angle

Table 6 Low salinity brine injections

Core	Oil	Water	V_w		ΔQ_o (%)	ΔP (kPa)	S_{ro} (%)
			(ml)	(PV)			
BW0	Mine.	Low sal	360	25.4	0	77.1	46.1
BW1	Crude	Low sal	399	27.3	0.4	27.6	38.4
BW2	Crude	Low sal	410	29.3	0.8	15.6	44.7
BW3	Crude	Low sal	446	24.3	1.2	4.1	42.3

saturation (BW0). Increased oil recoveries (ΔQ_o) in PV were 0, 0.4, 0.8, and 1.2% from cores BW0, BW1, BW2, and BW3, respectively. The injection pressure differences (ΔP) were 77.1, 27.6, 15.6, and 4.1 kPa for the respective cores at their new residual oil saturations (S_{or}) in this stage. No clay fines were produced.

4.2.2 Distilled Water Injections

Injections of distilled water (0 ppm) at a constant water injection rate (q_w) of 0.3 ml/min at 22°C were conducted after low salinity brine injections terminated (Fig. 5 and Table 7). The injected volumes of distilled water (V_w) were 367–401 ml (25.9–28.6 PVs) to ensure no further oil production from the cores. Note that the order of enhanced oil recoveries associated with distilled water injections was reversed. The high increased recovery was obtained from

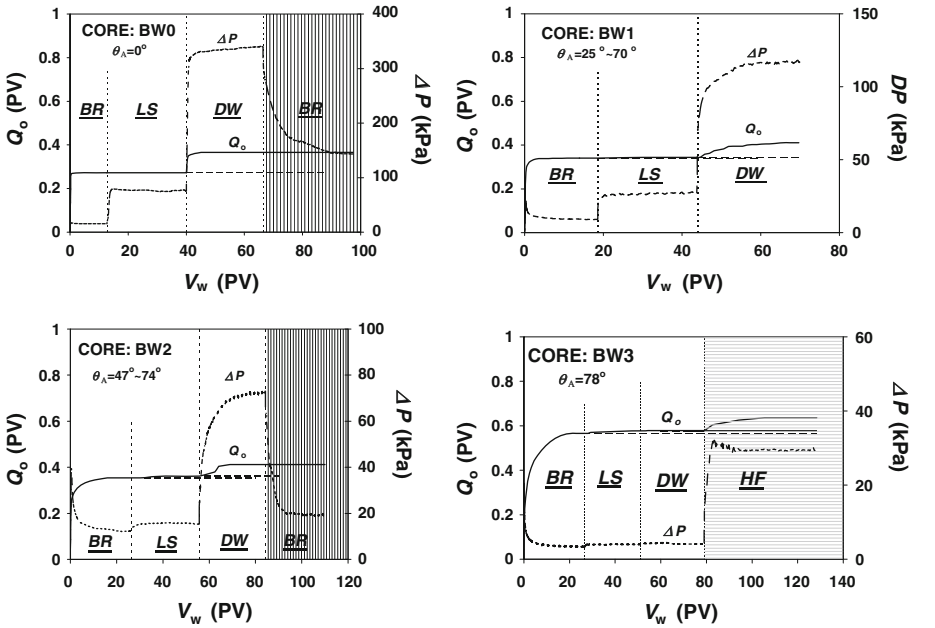

Fig. 5 The performance of secondary oil recovery associated with brine injection (BR) and tertiary oil recovery associated with low salinity brine injection (LS) and subsequent distilled water injection (DW), as well as the performance of brine injection (BR) following the distilled water injection or a high flow rate distilled water injection (HF) following the low flow rate distilled water injection. V_w is the cumulative volume of injected water in PV. Q_o is the cumulative oil recovery in PV and ΔP represents the injection pressure difference. θ_A represents the advancing contact angle

Table 7 Distilled water injections

Core	Oil	Water	V_w		ΔQ_o (%)	ΔP (kPa)	S_{ro} (%)
			(ml)	(PV)			
BW0	Mine.	Dist.	385	26.4	9.3	340	36.8
BW1	Crude	Dist.	367	25.9	6.6	117	31.8
BW2	Crude	Dist.	401	28.6	4.9	73	39.8
BW3	Crude	Dist.	391	28.2	0.1	4.5	42.1

the very strongly water-wet core with initial water saturation (BW0). Intermediate increased recoveries were obtained from the weakly water-wet cores with initial water saturations (BW1 and BW2). Low increased recovery was obtained from the very weakly water-wet core without initial water saturation (BW3). The increased oil recoveries (ΔQ_o) in PV were 9.3, 6.6, 4.9, and 0.1% from cores BW0, BW1, BW2, and BW3, respectively. The injection pressure differences (ΔP) were 340, 117, 73, and 4.5 kPa for the respective cores, at the new residual oil saturations (S_{or}) in this stage. Clay fines were produced from all cores during the distilled water injections, except for core BW3 that was originally completely saturated with crude oil.

Table 8 Brine injections after low salinity water Injections

Core	Oil	Water	V_w		ΔQ_o (%)	ΔP (kPa)	S_{ro} (%)
			(ml)	(PV)			
BW0	Mine.	Brine	452	31.0	0	144	36.8
BW2	Crude	Brine	352	25.1	0	19.7	39.8

Table 9 Distilled water injection at high flow rate after distilled water injection at low flow rate

Core	Oil	Water	V_w		ΔQ_o (%)	ΔP (kPa)	S_{ro} (%)
			(ml)	(PV)			
BW3	Crude	Dist.	385	49.2	5.7	29.5	36.4

4.3 Permeability Restoration Tests

To further understand how formation damage had been induced after the distilled water injections terminated, cores BW0 and BW2 were injected by brine (seawater) for the second time at the same flow rate in the same flow direction (Table 8). Injection without changing the flow rate and direction was designed to avoid hydraulically stirring the plugs formed by migrating clay fines. During each second brine injection, there was no further oil production (ΔQ_o) from either core. The injection pressure difference (ΔP) decreased quickly at the beginning of brine reinjection (Fig. 5). During each injection, suspension stopped being produced after about 25% PV brine was injected. In core BW0, which had been saturated with 0% asphaltic crude oil (73.4% mineral oil) before the secondary oil recovery operation, the injection pressure difference decreased from 340 to 144 kPa until 452 ml (31.0 PV) of brine was injected. The final injection pressure difference was still 9.3 times the injection pressure difference during the initial brine injection. In core BW2, which had been saturated with 80.9% asphaltic crude oil before the secondary oil recovery operation, the injection pressure difference decreased from 73 to 19.7 kPa until 352 ml (25.1 PV) of brine was injected. The final injection pressure difference was still 1.6 times the pressure difference during the initial brine injection. Both tests showed that the reduced permeability could be partially restored by reinjection of brine. The formation damage was more severe in core BW0, in which the saturated oil was mineral oil, thus, the core minerals, including clay crystals, had never been coated by asphaltene film.

4.4 High Flow Rate Injection

Core BW3, which had been completely saturated with asphaltic crude oil and aged before the secondary oil recovery operation (brine injection), was injected with 683 ml (49.2 PV) distilled water at a high water injection flow rate (q_w) of 3 ml/min after the distilled water injection at the low flow rate of 0.3 ml/min terminated. Oil production had stopped for 1.25 h during the low flow rate injection of distilled water (Fig. 5 and Table 9). All injections were conducted at 22°C. A further increased oil recovery (ΔQ_o) in PV of 5.7% was obtained under the higher injection pressure difference ($\Delta P = 29.5$ kPa) during the high flow rate injection of distilled water. No clay fines were produced during the high flow rate injection.

Table 10 Experimental values of viscosity and interfacial tension

Core	Brine injection		Distilled water injection	
	μ_w (mPa s)	σ (mN/m)	μ_w (mPa s)	σ (mN/m)
BW2	1.000	29.7	0.993	29.6

4.5 Measurements of the Viscosity of the Produced Water and the Interfacial Tension Between the Produced Crude Oil and Produced Water

The produced crude oil and water during distilled water injections into core BW2 were collected and analyzed to obtain the values of the water viscosity and the interfacial tension between crude oil and water (Table 10).

Compared with brine injection, no apparent alterations in the water viscosity and interfacial tension between the crude oil and water were observed during distilled water injection.

5 Analyses

5.1 Mechanism of the Secondary Oil Recovery Associated with Injection of Brine

In two cores with the same lithology, if wettability is the same, the secondary oil recovery (in PV) will be higher for the core with lower initial water saturation; if the initial water saturations are the same, the oil secondary recovery will be higher for the core with stronger oil-wetness.

As snap-off can readily happen in more-water-wet cores, the increased water saturation at and behind the water-invading front will be higher, thus the water-free recovery will be higher for those cores. The experimental data showed that the frontal saturations were 51.7, 41.2, 29.3, and 4.8% in cores BW0, BW1, BW2, and BW3, which are listed in the order of decreasing water-wetness. Correspondingly, the frontal saturations above the initial water saturations were 25.2, 14.0, 10.3, and 4.8% respectively (Fig. 6). Consequently, the corresponding BT recoveries were 26.0, 25.4, 19.3, and 15.1% in PV, respectively, for those cores.

As snap-off cannot readily occur in more-oil-wet cores, much of the continuous oil phase will not be disconnected for longer time and permit more continuous oil branches retreating in a piston-like manner along the porous channels. Therefore, for more-oil-wet cores, the saturation profile tends to bend upward after water BT for reaching a higher final recovery. The experiments showed that the final secondary recoveries in PV were 27.3, 34.0, 35.4, and 56.5%, respectively, for cores BW0, BW1, BW2, and BW3 (Fig. 6), which are listed in the order of decreasing water-wetness.

The above examples illustrate that the influence of wettability on secondary oil recovery can be quantitatively investigated by the newly introduced techniques.

5.2 Mechanism of Tertiary Oil Recovery Associated with Injection of Low Salinity Water (Including Low Salinity Brine and Distilled Water)

5.2.1 Excluded Reactions

5.2.1.1 No Apparent Viscosity and Interfacial Tension Alterations Judged by the laboratory measurements at different stages, we can directly determine whether the alteration of water

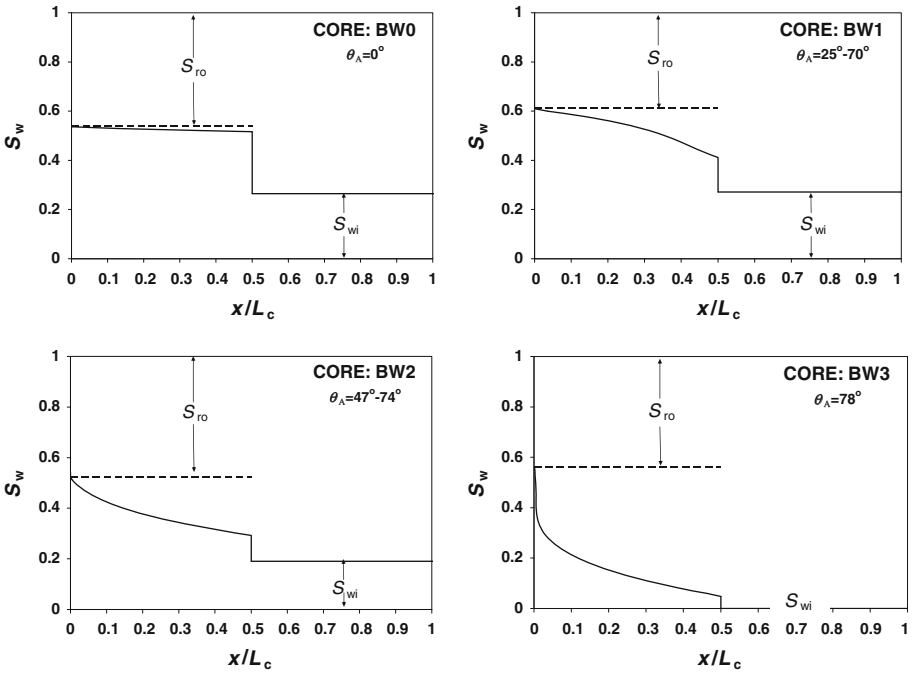

Fig. 6 Experimental saturation profiles during brine injections into Berea sandstone cores with different wettability. S_{wi} is the initial water saturation. S_{ro} is the residual oil saturation. θ_A represents the advancing contact angle. x is the distance and L_c is the core length. The profiles shown in the figures develop when the fronts are half way in the cores ($x/L_c = 0.5$)

viscosity or interfacial tension takes place during injection of low salinity water. As the measured viscosity and interfacial tension during distilled water injection were very close to their previous values during injection of brine (Table 10), it can be definitely concluded that no chemical reactions apparently affect the water viscosity and the interfacial tension between oil and water during injections of low salinity water.

Theoretically, during injections of low salinity water a few chemical reactions such as cation exchange (Lager et al. 2006; Lebedeva et al. 2009; Austad and Puntervold 2010) or saponification (McGuire et al. 2005) may take place to a certain degree, especially when an apparent change appears in the consequent pH values. However, none of them leads to a noticeable alteration in viscosity or interfacial tension as shown by experimental measurements.

5.2.1.2 No Favorable Wettability Alteration If the wettability alters toward increased waterwetness, it definitely plays a negative role in oil recovery associated with forced water injections. It cannot be emphasized too much while misleading is spreading.

The functions of convex interfaces and selloidal interfaces are different in secondary oil recovery. Convex interfaces can move faster due to spontaneous imbibition in more-water-wet rock but cannot cause disconnection of oil. Secondary oil recovery is only linked to the disconnection of oil by snap-off of selloidal interfaces. The more water-wet the pore, the lower the critical pore–throat aspect ratio will be, thus, more residual recovery will be obtained in more-water-wet cores. For example, when $\theta_A = 0°$, the critical pore–throat

aspect ratio $r_P/r_T = 1.49$; when $\theta_A = 60°$, the critical pore–throat aspect ratio $r_P/r_T = 1.75$ (Fig. 1). This is the reason why increased water-wetness is not favorable to secondary oil recovery. The influence of wettability on secondary oil recovery has also been demonstrated with systematic injection profiles in Sect. 5.1.

Moreover, increased water-wetness is not favorable to tertiary oil recovery either. Mobilization of an oil drop is comparatively difficult in a more-water-wet rock. This is because the difference between the capillary pressures generated by the downstream convex interface and upstream convex interface of an oil drop ($P_{cT} - P_{cP}$) will be greater if the rock becomes more water-wet. For example, if the downstream throat radius r_T is 20 μm, pore radius r_P is 50 μm and interface tension σ is 30 mN/m, when contact angle $\theta_R = \theta_A = 0°$, $P_{cT} - P_{cP} = 1,800$ Pa; when $\theta_R = 54°$ and $\theta_A = 60°$, $P_{cT} - P_{cP} = 1,163$ Pa. Although increased water-wetness can slightly help oil mobilization due to the fact that the disconnection of blobs is easier in the more-water-wet cores (Sects. 2.2 and 5.2.4), it is not the case where snap-off of blobs occurs on site during low salinity water injections. During low salinity water injections there is no enough time for invading low salinity water to alter the wettability in the area where the solid surface is covered by a trapped oil blob a moment ago.

In this study, we have obtained a direct experimental proof that the wettability alteration to increased water-wetness may not happen in tertiary oil recovery associated with low salinity water injection. The experiment showed that a high tertiary oil recovery associated with law salinity water injection was also obtained from the very strongly water-wet core (core BW0) during distilled water injection (Fig. 5). Because a very strongly water-wet core cannot become more water-wet, the possibility of wettability alteration to increased water-wetness can be excluded in this case.

The study of the cyclic brine and oil injections (Li 2010) (sequential waterflooding, as called by other authors lately) shows that injected brine can destroy the asphaltene films to allow pore walls to become more water-wet. As a result, less secondary oil recovery is obtained. This finding is confirmed by the succeeding tests where oil-wetness can be restored in the washed cores by resaturating with asphaltic crude oil and reaging. Using the data in the reference (Li 2010) and this article, we were able to make an estimation of wettability alteration due to washing. The analysis shows that, if the original advancing contact angle in a Berea sandstone core with permeability of 0.65 μm^2 is 50°, the reduction in advancing contact angle will be 2.5° after 10 PV of brine is injected at the flow rate of 0.3 ml/min at 20°C. The corresponding reduction in oil recovery will be less than 1.5% PV (the oil recovery reduction was partly due to plugging of porous network by colloidal asphaltenes in those tests). The above estimation came from two sources. One was the relationship between the oil recovery after BT (the range was from 10 to 38% PV) and the advancing angle (the range was from 0° to 78°). The other was the cumulative reduction in oil recovery (8% PV in total) for three cyclic brine and oil injections. Thus, the precision of the estimation is assured.

It can be expected that the wettability alteration to increased water-wetness caused by washing can also happen during injections of low salinity water. The alteration to more water-wetness due to washing is unfavorable to oil recovery during water injections.

Austad and Puntervold (2010) declared that desorption of organic material due to the reaction between protonated base and adsorbed acid may cause the desorbed area to become more water-wet during low salinity water injections. If this is true, the alternation to increased water-wetness will be stronger and oil recovery enhancement will become more difficult during low salinity water injections. A further study on the quantitative relation between wettability alteration and desorption is suggested.

Table 11 Water permeability during the sequential water injections

Core	$K_w(\mu m^2)$ in sequential water floods			
	First brine	Low salinity brine	Distilled water	Second brine
BW0	0.0196	0.0040	0.0009	0.0021
BW1	0.0310	0.0112	0.0026	
BW2	0.0249	0.0197	0.0042	0.0156
BW3	0.0880	0.0730	0.0665	

5.2.2 Water Permeability Reduction: The Only Dynamic Variable Which Induces Oil Mobilization During Low Salinity Injections

As three dynamic variables of the standard capillary number, viscosity, interfacial tension and wettability, have been excluded to be the active variables during the tertiary oil recovery associated with low salinity water injection, water permeability (K_w) is the only variable to be investigated at a fixed water injection flow rate for the tested cores (at a constant Darcy velocity).

It is rational to relate the permeability reduction during low salinity water injection to the plugging of porous network by clay. The direct proof is that during injections of distilled water into those cores which had not been completely saturated with crude oil, the injection pressure differences significantly increased and effluents with migrated kaolinite fines were produced while the water viscosities and water injection flow rate remained unchanged.

To make a quantitative analysis, a formula of water permeability (K_w) is needed. Rearranging the equation of the generalized Darcy's law for the water phase (Eq. 8), the required formula is immediately obtained and written as:

$$K_w = -q_w \frac{\mu_w L_c}{A \Delta P}. \tag{13}$$

The results calculated by Eq. 13 are listed in Table 11. The values of water permeability during the injections of low salinity brine (TDS is 1.78 g/l) are 20, 36, 79, and 83% of those during the injections of brine for the cores BW0, BW1, BW2, and BW3 originally saturated with 0, 72.8, 80.9, and 100% crude oil, respectively. The values of water permeability during the injections of distilled water (TDS is 0 g/l) are 5, 9, 17, and 76% of those during injections of brine for the respective cores.

As the water viscosity does not change and the flow rate of water injection is controlled constant, the increase of negative pressure gradient in water is only resulted by the reduction of water permeability during the injections of low salinity water (Fig. 7a). The initial crude oil saturation is directly correlated with the volume of clay coated by asphaltene films formed in the period of aging. In other words, there are two factors that control the reduction of water permeability in the cores with the same lithology. One is the quantity of uncoated clay and the other is the diluted salinity of the injected water. Both determine how low the water permeability can be reduced by clay plugging, thus, how high the negative pressure gradient can be raised by injection of low salinity water at a fixed flow velocity.

The hypothesis that migration of detached mixed-wet clay particles with absorbed residual oil drops (Tang and Morrow 1999) has no relevance to the standard capillary number. Their hypothesis claims that the increased recovery originates from those oil drops adhering

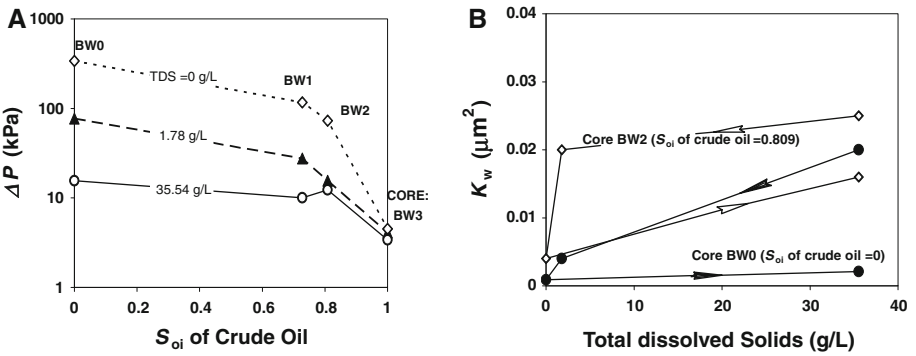

Fig. 7 Influence of salinity on injection pressure difference and water permeability. **a** shows the influence of the initial crude oil saturation (S_{oi} of crude oil) and salinity (shown by TDS) on the injection pressure difference (ΔP). Please note that ΔP is expressed on the logarithmic scale. **b** shows the change of water permeability (K_w) with the alteration of salinity in injected water (TDS)

to clay fines at pore walls, which is contradictory to the fundamental concept that residual oil is trapped due to capillary pressure actions. Several experiments (including "low salinity brine injections" reported in this article) have directly proven that the increased oil recovery associated with injection of low salinity water can be obtained without clay migration.

5.2.3 Influence of Salinity and Amount of Uncoated Clay on Water Permeability

As the systematic experiments show, the increased injection pressure difference is not only related to the salinity of injected water, but also to the initial crude oil saturation (Fig. 7a).

It is heuristic that the order of the tertiary oil recoveries associated with low salinity water injection from similar cores with different wettability was reversed as the salinity of the injected water decreased. The experiments show that the highest oil recovery associated with injection of low salinity water was obtained from the core initially saturated with 100% asphaltic crude oil when the salinity was relatively high (Sect. 4.2.1), while the highest oil recovery associated with injection of low salinity water was obtained from the core initially saturated with 0% asphaltic crude oil (73.4% mineral oil) when the salinity was very low (Sect. 4.2.2). The order reversal is due to the fact that oil-wetness is an increasing function of the initial asphaltic crude oil saturation, while the amount of uncoated clay is a decreasing function of the initial asphaltic crude oil saturation. Therefore, the highest oil recovery associated with injection of low salinity water may be obtained from the core initially saturated with a part of asphaltic crude oil and a part of brine when the salinity is neither high nor low. This case has been frequently reported previously. In conclusion, tertiary oil recovery associated with low salinity water injection is affected by three factors, the amount of uncoated clay, salinity and wettability, during low salinity water injections at the common laboratory flow rate. Of course, tertiary oil recovery associated with low salinity water injection is always affected by flow velocity.

The above experiments disproved the hypothesis that increased oil recovery is only related to mixed wettability during injections of low salinity water (Zhang and Morrow 2006; Loahardjo et al. 2007). The mixed wettability hypothesis is unscientific, because it is assumed to behave according to the distribution of water and oil within the asphaltic crude oil reservoirs. As we know, wettability results from intermolecular interactions and during water injections the oil-water interfaces move within the spaces originally occupied by the oil phase. There-

fore, no adhesive and cohesive forces on the solid surfaces covered by the connecting water can affect the distant interfaces which are driving or disconnecting the continuous oil phase (Li 2010).

Further, as the increased injection pressure shows, water can still contact some clay minerals, even if all of them may be considered to be completely coated by asphaltene film in the aged core initially saturated with 100% asphaltic crude oil (core BW3).

Injections of brine were conducted following injections of distilled water. The results revealed that the water permeability (K_w) reduced by low salinity water could be partially recovered by reinjection of brine (Fig. 7b). For core BW0, which had been initially saturated with 0% asphaltic crude oil (73.4% mineral oil) before the secondary oil recovery operation, the water permeability during the secondary brine injection was 2.4 times that during the previous injection of distilled water, but was only 11% of that during the primary brine injection. For core BW2, which had been initially saturated with 80.9% asphaltic crude oil before the secondary oil recovery operation, the water permeability during the secondary brine injection was 3.7 times that during the previous injection of distilled water, but was still 62% of that during the primary brine injection. Therefore, it can be concluded that if less clay is coated by asphaltene films in the cores with the same lithology, formation damage will be more severe during low salinity water injections.

It is generally believed that kaolinite does not absorb water, so it does not swell when coming in contact with low salinity water. Thus, the permeability decrease has been attributed to the migration of kaolinite (Gray and Rex 1966). We have observed that clay fines were produced during distilled water injections. Hence, there is no question that fresh water with the migrating clay particles and crystals can cause the reduction of water permeability. However, the increased pressure difference was not accompanied with production of clay fines during injections of low salinity brine (1,780 ppm). In addition, the permeability reduced by low salinity water can be partially recovered by injection of brine. Both phenomena should be related to on-site volumetric alteration of the kaolinite aggregates.

5.2.4 Influence of Interfacial Tension and Wettability on the Tertiary Oil Recovery Associated with Low Salinity Water Injection

As shown by the equation of standard capillary number, low interfacial tension and strong oil-wetness can always benefit tertiary oil recovery associated with water injection. Because the interfacial tension is not changed and the alteration to a more-water-wet condition is unfavorable to recovery and not important compared with the alteration of pressure difference, the interfacial tension and wettability cannot be considered as the causes but the conditions of tertiary oil recovery associated with injection of low salinity water. Now let us make an analysis to quantitatively determine the influence of interfacial tension and wettability on the tertiary oil recovery associated with injection of low salinity water. The range of interfacial tension in our laboratory is between 29.7 and 48.8 mN/m and the range of advancing contact angle in our laboratory is between 0° and 78°.

Combining Eqs. 12, 13 and $V = q_w/A$, we obtained

$$N_c L_c = -\frac{\Delta P}{\sigma \cos \theta_R}. \tag{14}$$

The range of the final tertiary oil recoveries ΔQ_o^* in our experiments is from 5.7 to 9.3% with an average value of 7.3%. Because none of the values of the investigated ΔQ_o^* is very different from the average of the final tertiary oil recoveries (ΔQ_o), we can calculate ΔP

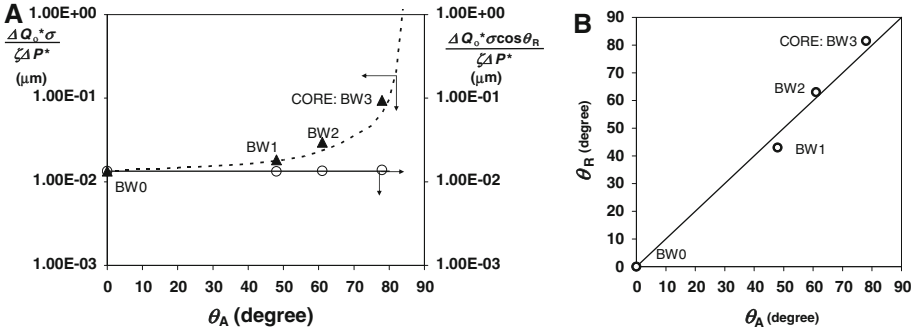

Fig. 8 Measurement of receding contact angle inside cores. **a** shows the influence of wettability and interfacial tension on tertiary oil recovery. $\Delta Q_o^* \sigma / \zeta \Delta P^*$ at θ_A is related to the curvature radii of upstream and downstream interfaces corresponding to tertiary recovery of 7.3% PV while $\Delta Q_o^* \sigma \cos\theta_R / \zeta \Delta P^*$ at θ_A is related to the radii of pore and throat of the capillary trap corresponding to tertiary recovery of 7.3% PV. **b** shows the measured receding contact angles (θ_R) compared with the measured corresponding advancing contact angles (θ_A)

(the injection pressure difference corresponding to ΔQ_o (=the tertiary oil recovery of 7.3% PV)) for any core by the following equation:

$$\Delta P = \frac{\Delta Q_o}{\Delta Q_o^*} \Delta P^*, \tag{15}$$

where ΔP^* is the injection pressure difference corresponding to the final tertiary oil recovery ΔQ_o^* for any core. Substituting Eq. 15 into Eq. 14, we obtain:

$$\frac{\Delta Q_o^*}{\Delta P^*} \sigma \cos\theta_R = \Delta Q_o / N_c L_c. \tag{16}$$

Using symbol N_c^0 to denote the standard capillary number at the tertiary oil recovery of 7.3% PV (ΔQ_o) for core BW0 in which $\theta_R = \theta_A = 0$ and using symbol N_c to denote the standard capillary number at the tertiary oil recovery of 7.3% PV (ΔQ_o) for any other core with $\theta_R > 0$, we may define the relation between N_c^0 and N_c as:

$$N_c^0 = \zeta N_c, \tag{17}$$

where ζ is the ratio of N_c^0 to N_c at the tertiary oil recovery of 7.3% PV (ΔQ_o).

Combining Eqs. 16 and 17 yields:

$$\Delta Q_o / N_c^0 L_c = \frac{\Delta Q_o^*}{\zeta \Delta P^*} \sigma \cos\theta_R \quad \text{when} \quad \theta_A > \theta_R > 0^\circ \tag{18}$$

and

$$\Delta Q_o / N_c^0 L_c = \frac{\Delta Q_o^*}{\Delta P^*} \sigma \quad \text{when} \quad \theta_A = \theta_R = 0^\circ. \tag{19}$$

In both above equations, ΔQ_o and N_c^0 are two constants and L_c can be taken as a constant because the lengths of the tested cores are almost the same. Therefore, the θ_R corresponding to the measured median of θ_A for any studied core with $\theta_A > \theta_R > 0$ can be obtained by combining Eqs. 18 and Eq. 19. The calculated results are plotted in Fig. 8 or listed in Table 12.

In Fig. 8a, the relationship between $\Delta Q_o^* \sigma / \zeta \Delta P^*$ and θ_A shows the influence of interfacial tension and wettability on the tertiary oil recovery. The term of $\Delta Q_o^* \sigma / \zeta \Delta P^*$ is related

Table 12 Contact angles measured from the data of flow performances

Core	θ_A	θ_R	Hysteresis
BW0	0°	0°	0°
BW1	48°	43°	−5°
BW2	61°	63°	2°
BW3	78°	81.5°	3.5°

Table 13 Tertiary oil recoveries versus standard capillary numbers during low salinity water injections

Core	ΔQ_o in PV	μ (Pa s)	V (m/s)	K_w (m^2)	σ (N/m)	Θ_R (°)	N_c (m^{-2})
BW0	0.000	0.001	4.73×10^{-6}	3.97×10^{-15}	0.0488	0	2.4×10^{7}
	0.093	0.00099	4.73×10^{-6}	9.01×10^{-16}	0.0488	0	1.1×10^{8}
BW1	0.004	0.001	4.80×10^{-6}	1.75×10^{-14}	0.0297	43	2.0×10^{7}
	0.07	0.00099	4.80×10^{-6}	2.65×10^{-15}	0.0297	43	8.3×10^{7}
BW2	0.008	0.001	4.83×10^{-6}	1.97×10^{-14}	0.0297	63	1.8×10^{7}
	0.057	0.00099	4.83×10^{-6}	4.20×10^{-15}	0.0297	63	8.4×10^{7}
BW3	0.012	0.001	4.80×10^{-6}	7.30×10^{-14}	0.0297	81.5	1.5×10^{7}
	0.014	0.00099	4.80×10^{-6}	6.65×10^{-14}	0.0297	81.5	1.6×10^{7}
	0.071	0.00099	4.80×10^{-5}	8.65×10^{-14}	0.0297	81.5	1.1×10^{8}

to the curvature radii of the upstream and downstream interfaces of the residual oil drop being mobilized at the tertiary oil recovery of 7.3% PV (ΔQ_o). In Fig. 8a, when θ_A is 0°, the value of $\Delta Q_o^* \sigma / \zeta \Delta P^*$ is the lowest; when θ_A is close to 90°, the value of $\Delta Q_o^* \sigma / \zeta \Delta P^*$ is going to be infinite. The curve demonstrates that less external energy will be required for the same tertiary oil recovery if the contact angle is great and/or the interfacial tension is low. On the other hand, the term of $\Delta Q_o^* \sigma \cos\theta_R / \zeta \Delta P^*$ is related to the radii of pore and throat of the capillary trap for the residual oil drop being mobilized at the tertiary oil recovery of 7.3% PV (ΔQ_o).

If all results were perfect, each point should have been located under the "diagonal" in Fig. 8b, except for the point at the origin. However, two points are not. Analytically, the estimated errors of measured contact angles are about five degrees for the two measurements. The errors may be caused by the difference in the original residual oil distribution and clay plugging degree, as well as by the wettability assignment (Sect. 4.1.1). Two types of contact angles were measured independently from spontaneous imbibition and forced injection experiments so that both types of contact angles are equally qualified due to their good correlation. No other measurements of advancing and receding contact angles have been achieved inside the cores in the past.

Using the measured θ_R (Table 12 and Fig. 8), we finally obtained the relationship between tertiary oil recovery (ΔQ_o) and the standard capillary number ($N_c = \mu V / (K_w \sigma \cos\theta_R)$) (Table 13 and Fig. 9) for injections of low salinity water. Please note that ΔQ_o in Table 13 and Fig. 9 represents a cumulative tertiary oil recovery (ΔQ_o there does not represent the tertiary oil recovery of 7.3% PV as it does in Eqs. 15–19).

Three important conclusions can be drawn from the resulting experimental curves (ΔQ_o versus N_c). Two of them agree with the theory described in Sect. 2.2.

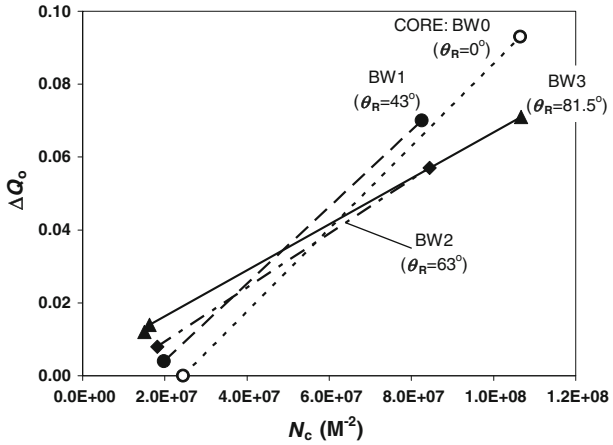

Fig. 9 Relationship between the tertiary oil recovery (ΔQ_o) in PV and the standard capillary number (N_c). θ_R represents the receding contact angle

(1) At a fixed wettability, the higher the standard capillary number (N_c), the more the tertiary oil recovery (ΔQ_o) will be.
(2) The more oil-wet the core behaves, the less the curve gradient ($\Delta Q_o/N_c$) will be, which is supposed to be related to the disconnection of blobs. The curve gradients ($\Delta Q_o/N_c$) are 11.3×10^{-10}, 10.5×10^{-10}, 7.4×10^{-10} and 6.3×10^{-10} m^2 corresponding to θ_R of 0°, 43°, 63° and 81.5° respectively.
However, the following conclusion seems to disagree with the theory.
(3) At a low tertiary oil recovery, the more oil-wet the core behaves, the lower the dynamic value of the standard capillary number (N_c) will be required.

According to the theory described in Sect. 2.2, the hysteresis of contact angle corresponding to weak water-wetness causes the resistance against mobilization in capillary trap (the left-hand side of Eq. 11) to be slightly higher for the same oil drop in the same trap so that the "theoretical" ΔQ_o versus N_c curves for weak water-wetness should be on the right-hand side of that for very strong oil-wetness. However, in our experiments, more uncoated clay existed in the more-water-wet cores. Thus, more throats of capillary traps became narrower in the more-water-wet core owing to clay plugs created during injections of low salinity water. This is the reason why the order of the "practical" curves was partially reversed. Consequently, an important deduction can be drawn from these "unexpected" experimental results that some or all capillary traps can become more severe obstacles in any clay-bearing sandstone core or any clay-bearing sandstone formation during low salinity water injections. Note that this deduction agrees with the theory described in Sect. 2.2 and will be mentioned in Sect. 5.2.6.

The phenomenon that mobilization of residual oil starts at a critical capillary number has been repeatedly observed in early researches (Chatzis and Morrow 1984; Wardlaw and McKellar 1985; Wardlaw 1988). An additional proof of the threshold for production of discontinuous oil was obtained in this study. Data showed that no oil was recovered from the very strongly water-wet core BW0 ($\theta_A = 0^o$) during the tertiary oil recovery associated with injection of low salinity brine. The corresponding injection pressure difference was 4.9 times that during the secondary oil recovery associated with injection of brine (Fig. 5). However, 9.3% oil in PV was obtained from core BW0 during the succeeding injection of distilled water. The corresponding injection pressure difference was 21.8 times that in sec-

ondary oil recovery associated with injection of brine. Please note that for the low salinity water injections the onset of mobilization cannot be judged by the dimensionless capillary number ($Ca = \mu V/\sigma$) but can be judged by the standard capillary pressure number ($N_c = \mu V/(K_w \sigma \cos\theta_R)$) (Fig. 9).

In Fig. 9, the values of the critical standard capillary number (N_c) for onset of mobilization are 3.0×10^7, 1.6×10^7, 1.0×10^7 and $5.0 \times 10^6\ m^{-2}$ corresponding to θ_R of 0°, 43°, 63° and 81.5° respectively. The values of the equivalent critical dimensionless capillary number (C_a) for onset of mobilization in the unplugged cores are 5.9×10^{-7}, 3.6×10^{-7}, 1.1×10^{-7}, and 5.6×10^{-9} corresponding to θ_R of 0°, 43°, 63° and 81.5° respectively.

5.2.4.1 An additional remark: Secondary Oil Recovery Mechanism of Low Salinity Water Injection As the tertiary oil recovery associated with low salinity water injection only relates to clay plugging, the mechanism of the increased secondary oil recovery (EOR in secondary oil recovery) associated with low salinity water injection must be the same, except that the recovered discontinuous oil is obtained due to the prevention of the entrapment of some newly formed oil drops rather than the mobilization of some trapped oil drops. For simplification, we will still call the escaping oil drops in secondary oil recovery the mobilized oil drops. Compared to brine injection at the same flow velocity, the increased secondary oil recovery associated with injection of low salinity water should be equal to the tertiary oil recovery associated with injection of low salinity water from a similar core with the same initial condition of secondary oil recovery.

5.2.5 Influence of Flow Velocity on Tertiary Oil Recovery Associated with Low Salinity Water Injection

Tertiary oil recovery is strongly related to flow velocity. An additional experimental proof has been obtained in this study for the tertiary oil recovery associated with injection of low salinity water. When the flow rate of distilled water injection increased 10 times, 5.7% increased oil recovery in PV was obtained from core BW3 ($\theta_A = 78^o$) after oil production had stopped for 1.25 h during the distilled water injection at the low flow rate. Only 1.4% increased oil recovery in PV had been obtained from core BW3 after low salinity brine and distilled water injections at the low flow rate. Note that the injection pressure at the high flow rate was only as high as 6.6 times that at the low flow rate. This is because the residual saturation decreased from 42.1 to 36.4% during the distilled water injection at the high flow rate (refer to water permeability explanation in Sect. 2.2).

Although the phenomenon that tertiary oil recovery is strongly related to flow rate has long been observed (Chatzis and Morrow 1984; Wardlaw and McKellar 1985), this fact was neglected in the recently published articles when dealing with the tertiary oil recovery associated with injection of low salinity water (Zhang and Morrow 2006; Loahardjo et al. 2007).

Similar to tested distilled water injections at different flow velocities, discontinuous oil can also be mobilized by brine injection either in secondary or tertiary oil recovery, if the flow velocity is high enough. This is an essential physics in EOR that will be mentioned in Sect. 5.2.6.

To correctly evaluate the reservoir recovery associated with injection of low salinity water, some essential knowledge related to flow rate and flow acceleration is introduced: (1) Because the flow is fastest in the oil formation in near wellbore regions, the highest reduction in oil saturation caused by injection of low salinity water will occur there. Therefore, it is almost impossible that the EOR associated with low salinity water injection for a core can be as much as that for a reservoir in near wellbore region, where the flow velocity is generally

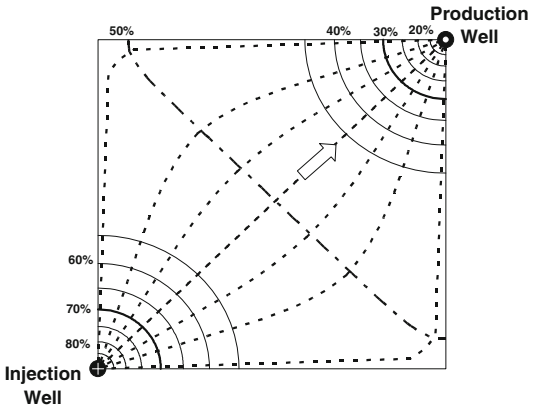

Fig. 10 Equal-pressure contours and streamlines in a quadrant of a five-spot-network element during one phase flow (according to Muskat and Wyckoff 1934). Percentage represents the total pressure drop. The *arrow* shows the flow direction. The *dashed line plus dots* represents the equal-pressure contour where the flow velocity is lowest along flow lines. The heavy *solid lines* show two equal-pressure contours where flow rate is the same, but the sign of the flow velocity gradient at contour 70% (negative) is different from that at contour 30% (positive)

about one order of magnitude higher (refer to the first paragraph in Sect. 5.2.5). (2) Because the flow decelerates as it is away from the injection well, part or all of the mobilized oil drops will be trapped again. Conversely, the flow accelerates at half way between the injection and production wells so that there is no re-trap in the acceleration zone if the mobilization occurs there. (3) If there is a zone where the flow velocity is lower than that for the onset of oil mobilization, the mobilized oil cannot pass it.

Please note that the deceleration problem is unavoidable in tertiary oil recovery and will be introduced in the following calculation outlines.

5.2.5.1 In the Case Where the Lowest Darcy Velocity is Higher Than the Velocity for the Onset of Oil Mobilization We will make the analysis using the Darcy velocity (V) instead of the standard capillary number, (N_c). $V$is proportional to N_c for the homogenous formation with uniform thickness.

If any Darcy velocity in the whole reservoir is higher than the velocity for the onset of oil mobilization, the EOR between the injection well and the lowest-velocity line (50% equal-pressure contour as shown in Fig. 10 (according to Muskat and Wyckoff 1934), for example) is equal to the EOR estimated at the lowest-velocity line. This is because re-trap happens in the zone where the flow velocity decelerates (between 100% equal-pressure contour and 50% equal-pressure contour in Fig. 10 for the example). The EOR between the production well and the lowest flow velocity line is higher than the EOR estimated at the lowest-velocity line. This occurs because the standard capillary number continuously increases along the flow lines from the lowest velocity points to the production well. According to the above criteria, an EOR map corresponding to the feasible water injection flow rate for the objective reservoir can be made from the experimental data. The reservoir EOR should be calculated by integration on that map.

5.2.5.2 In the Case Where the Lowest Darcy Velocity is Lower than the Velocity for the Onset of Oil Mobilization The critical flow velocity line is the equal-velocity line (corresponding to an equal-pressure contour if formation thickness and permeability are the same) where the Darcy velocity is just high enough for the onset of oil mobilization. In the case

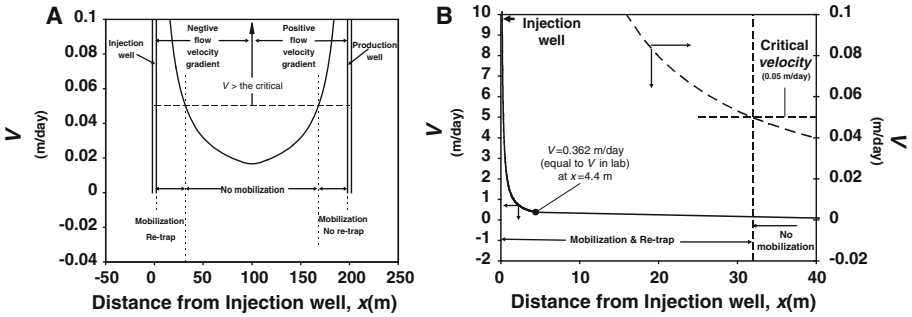

Fig. 11 Divisions of mobilization and re-trap in a reservoir. **a** shows that the produced mobilized oil can only come from the division on the right-hand side due to both favorable conditions: flow velocity above the critical for mobilization and positive flow velocity gradient. No mobilized oil can pass through the zone in the middle, where the flow velocity is lower than that for onset of mobilization. A part of the detailed **a** is illustrated by **b**. **b** shows that the flow velocity in the region near the injection wellbore can be two orders of magnitude higher than the critical flow velocity. The reduction in oil saturation is greatest in the regions near the injection wellbore due to the highest flow velocity.

where the lowest Darcy velocity is lower than the velocity for onset of oil mobilization, the reservoir EOR can be obtained only from the area between the production well and the critical flow velocity line on the downstream side (30% equal-pressure line in Fig. 10, for example). This is because the zone where flow velocity is lower than the critical one (between 30 and 70% equal-pressure lines in Fig. 10 for the example) prevents any mobilized oil drops from passing it. In this case, the reservoir EOR should also be calculated by integration on the EOR map.

The divisions of mobilization and re-trap in a reservoir cross section are illustrated in Fig. 11. The adopted injection rate of low salinity water for each meter of depth is $10\,m^3$/day, which is a high value for the clay-bearing sandstone reservoirs. As a result, the apparent flow velocity, V, at 4.4 meters from the center of the injection well is equal to the velocity commonly controlled in the laboratory (0.362 m/day). If all data are the same as the data of core, BW2 (0.686 Darcy), the EOR for the five-spot-network element shown by Fig. 10 will be 0.03% of PV as calculated by integration on the EOR map. The data of core BW2 (Table 13 and Fig. 9) are the following: $\mu_w = 0.001$ Pa.s, $K_w = 4.2 \times 10^{-15}\,m^2$, $\sigma = 0.0297$N/m, $\theta_R = 63°$, and the critical N_c for mobilization $= 10^7\,m^{-2}$. Additionally, the N_c is $8.4 \times 10^7\,m^{-2}$ corresponding to laboratory EOR (ΔQ_o) of 5.7% PV during the distilled water injection, which is much higher than EOR using a natural low salinity water. Even supposing that the laboratory EOR (ΔQ_o) could be 20% PV as reported by (Loahardjo et al. 2007), the EOR for the reservoir element would only be as much as 0.11% PV, which would still be very low. The calculations show that probably no commercial EOR can be obtained in any reservoir by injections of low salinity water in either secondary or tertiary oil recovery mode.

In the following section, the negative evaluations on low salinity water injection are made regardless of how high an experiment EOR may be obtained by injection of low salinity water.

5.2.6 Final Remarks

Injection of low salinity water has been recommended for a decade merely because higher oil recovery can be obtained by injection of low salinity water, compared with injection of

brine at same flow velocity in the same clay-bearing sandstone. However, the truth is that the highest oil recovery can only be obtained by injection of brine in the clay-bearing sandstone reservoirs.

We have known that the discontinuous oil can be mobilized during low salinity water injection at the fixed flow velocity simply because the water injection pressure has to be remarkably raised due to clay plugging. However, when the water injectivity index for low salinity water is much lower than that for brine, the equivalent injection pressure, not the equivalent flow velocity, must be taken as the precondition in comparing the reservoir recoveries associated with different salinity water injections. This is because the water injection pressure cannot be raised without limit in the field operations, otherwise the over elevated injection pressure will cause hydraulic fracturing and water will move off along fractures reducing or ceasing the effectiveness of the recovery process.

Actually, the pressure gradient in the flooded formation can be upheld higher not only by reducing the water permeability while low salinity water is injected (Sect. 5.2.2), but also by increasing water injection rate while brine is injected (Sect. 5.2.5). As suggested by the relation among flow velocity, water permeability, and pressure difference by the generalized Darcy's law (Eq. 8), the same pressure gradient can be set up by both water injections at the same water injection pressure in a clay-bearing reservoir. However, the plugging of porous network caused by low salinity water is unfavorable for mobilization of the discontinuous oil (Sect. 5.2.4). Therefore, the highest oil recovery from any clay-bearing reservoir can only be achieved by injection of brine at the maximum permitted injection pressure. In addition, as the maximum permitted injection rate for brine is higher in a clay-bearing reservoir, the consequential oil recovery period will be shorter. Therefore, the previously claimed superiority of low salinity water injection over brine injection cannot be supported.

6 Conclusions and Suggestions

The oil recovery mechanism of low salinity water injection is comprehensively disclosed through systematic experiments guided by the fundamental recovery theories. The important conclusions and suggestions are as follows:

1. In either secondary or tertiary oil recovery, the EOR associated with injection of low salinity water is obtained under a negative pressure gradient higher than that during the brine injection at the same flow velocity, as the water permeability is reduced due to blockage of porous network by swelling clay aggregates or migrating clay particles and crystals.
2. The experiments proved that the EOR associated with injection of low salinity water is influenced by the amount of clay uncoated by asphaltene films, salinity of injected water, and wettability of sandstone. Contrary to the previous reports, the EOR by low salinity water injection can also be obtained from both very strongly water-wet cores and very weakly water-wet cores at the common laboratory Darcy velocity.
3. For injection of low salinity water, the EOR is strongly dependent on flow velocity and flow acceleration. When flow decelerates, some or all mobilized oil drops will be trapped again. Therefore, for injection of low salinity water, the reservoir EOR must be calculated by integration on the EOR map based on the laboratory relationship between EOR and the flow velocity and the criteria of re-entrapment associated with the flow acceleration. All data for plotting the map must be obtained from the

experiments based on the well-modeled characteristics of the relevant reservoir and the available water.

4. In practice, injection of brine should be the first option for a clay-bearing reservoir, because greater oil recovery can be obtained by using brine under the maximum permitted injection pressure. Injection of low salinity water into a clay-bearing reservoir should only be considered in the case where other more saline water is not available. This is because injection of low salinity water can always cause less EOR and prolong the recovery period in a clay-bearing reservoir. Particularly, low salinity water may cause serious injection problems in some clay-bearing reservoirs.
5. The standard capillary number and its interpretations presented in this article are very useful for further studies of tertiary oil recovery. Lower interfacial tension, stronger oil-wetness, lower water permeability, higher water viscosity, or higher Darcy velocity is supportive to create a higher dynamic standard capillary number. The deceleration problem is unavoidable in tertiary oil recovery, so sufficient attention must be paid to it when dealing with EOR.

References

Austad, T., Puntervold, T.: Chemical mechanism of low salinity water flooding in sandstone reservoirs. SPE 129767, Presented at SPE improved oil recovery symposium, 24–28 April 2010, Tulsa, OK (2010)

Chatzis, I., Morrow, N.R.: Correlation of capillary number relationships for sandstones. SPEJ. **24**, 555–562 (1984)

Gardescu, I.I.: Behavior of gas bubbles in capillary spaces. Trans. AIME **86**, 351–369 (1930)

Gray, D.H., Rex, R.W.: Formation damage in sandstones caused by clay dispersion and migration. Clay Clay Miner. **34**, 355–366 (1966)

Jamin, J.M.: Memoir on equilibrium and movement of liquids in porous substances. Compt. Rend. **50**, 172–176, 311–314, 385–389 (1860)

Lager, A., Webb, K.J., Black, C.J.J., Singleton, M., Sorbie, K.S.: Low salinity oil recovery—an experimental investigation. In: Proceedings of International Symposium of the Society of Core Analysts, Trondheim, Norway, September 2006

Lager, A., Webb, K.J., Black, C.J.J: Impact of brine chemistry on oil recovery. A24, Presented at the 14th European symposium on IOR, Cairo, Egypt, April 2007

Lebedeva, E., Senden, T.J., Knackstedt, M., Morrow, N.R.: Improved oil recovery from tensleep sandstone—studies of brine-rock interactions by micro-CT and AFM. Presented at the 15th European symposium of improved oil recovery, Paris, 27–29 April 2009

Li, Y.: Rebuting enhanced oil recovery by cyclic water and oil floods. SPE 133154, presented at Trinidad and Tobago energy resources conference, 27–30 June 2010, Port of Spain, Trinidad (2010)

Li, Y.: Analytical solutions for linear counter-current spontaneous imbibition in the frontal flow period. Transp. Porous Media **86**(3), 827–850 (2011)

Li, Y., Wardlaw, N.C.: The Influence of wettability and critical pore-throat size ratio on snap-off. J. Colloid Interface Sci. **109**(2), 461–472 (1986a)

Li, Y., Wardlaw, N.C.: Mechanisms of non-wetting phase trapping during imbibition at slow rates. J. Colloid Interface Sci. **109**(2), 473–485 (1986b)

Li, Y., Laidlaw, W.C., Wardlaw, N.C.: Sensitivity of drainage and imbibition to pore structure as revealed by computer simulation of displacement process. Adv. Colloid Interface Sci. **26**, 1–68 (1986)

Li, Y., Ruth, D., Mason, G., Morrow, N.R.: Pressures acting in counter-current spontaneous imbibition. JPSE **52**(1–4), 87–99 (2006)

Li, Y., Morrow, N.R., Mason, G., Ruth, D.: Capillary pressure at the imbibition front during water-oil counter-current spontaneous imbibition. Transp. Porous Media **77**, 475–487 (2009)

Ligthelm, D.J, Gronsveld, J., Hofman, J.P., Brussee, N.J., Marcelis, F., van der Linde, A.J.: Novel waterflooding strategy by manipulation of injection brine composition. SPE 119835, presented at SPE EUROPEC/EAGE annual conference and exhibition, June 2009

Loahardjo, N., Xie, X., Yin, P., Morrow, N.R.: Low salinity waterflooding of a reservoir rock. In: Proceedings of the 2007 International Society of Core Analysts Meeting, Calgary, Canada, September 2007

McGuire, P.L., Chatham, J.R., Paskvan, F.K., Sommer, D.M., Carini, F.H.: Low salinity oil recovery: an exciting new EOR opportunity for Alaska's North Slope. In: SPE 93903 in Proceedings of SPE Western Regional Meeting, Irvine, CA, April 2005

Melrose, J.C., Brandner, C.F.: Role of capillary forces in determining microscopic displacement efficiency for oil recovery by waterflooding. J. Can. Pet. Technol. **13**(4), 54–62 (1974)

Moore, T.F., Slobod, R.L.: The effect of viscosity and capillarity on the displacement of oil by water. Prod. Mon. **20**, 20–30 (1956)

Muskat, M., Wyckoff, R.D.: A theoretical analysis of waterflooding networks. Trans. AIME **107**, 62–77 (1934)

Sorbie K.S., Collins I.R.: A proposed pore-scale mechanism for how low salinity waterflooding works. SPE 129833, presented at SPE improved oil recovery symposium, 24–28 April 2010, Tulsa, OK (2010)

Tang, G.Q., Morrow, N.R.: Salinity, temperature, oil composition and oil recovery by waterflooding. SPE Reserv. Eng. **12**(4), 269–276 (1997)

Tang, G., Morrow, N.R.: Influence of brine composition and fines migration on crude oil/brine/rock interactions and oil recovery. J. Pet. Sci. Eng. **24**, 99–111 (1999)

Wardlaw, N.C.: Effects of capillary number and its component variables on waterflood efficiency and oil mobilisation. AOSTRA J. Res. **4**, 35–43 (1988)

Wardlaw, N.C., McKellar, M.: Oil blob populations and mobilization of trapped oil in unconsolidated packs. Can. J. Chem. Eng. **63**:525–532 (1985). Full text via cross ref view record in Scopus cited by in Scopus (29) (1985)

Webb, K.J., Black C.J.J., Al-Ajeel H.: Low salinity oil recovery—log-inject-log. In: SPE 89379 in Proceedings of SPE/DOE Fourteenth Symposium on Improved Oil Recovery, Tulsa, OK, April 2004

Webb K.J., Black C.J.J., Edmonds I.J.: The role of reservoir condition corefloods. Paper in the 13th European symposium on improved oil recovery, Budapest, Hungary, April 2005

Welge, H.J.: A simplified method for computing oil recovery by gas or water drive. Trans. AIME **195**, 91–98 (1952)

Zhang, Y., Morrow N.R.: Comparison of secondary and tertiary recovery with change in injection brine composition for crude oil/sandstone combinations. In: SPE 99757 in Proceedings of SPE/DOE Symposium on Improved Oil Recovery, Tulsa, OK, April 2006